Compton Scattering off polarized electrons with a High Finesse Fabry-Pérot Cavity at JLab

N. Falletto, M. Authier, M. Baylac, M. Boyer, F. Bugeon, E. Burtin, C. Cavata, N. Colombel, G. Congretel, R. Coquillard, G. Coulloux, B. Couzy, P. Deck, A. Delbart [1], D. Desforges, A. Donati, B. Duboué, S. Escoffier, F. Farci, B. Frois, P. Girardot, J. Guillotau, C. Henriot, C. Jeanney, M. Juillard, J-P. Jorda, P. Legou, D. Lhuillier, Y. Lussignol, Ph. Mangeot, X. Martin, F. Marie, J. Martino, M. Maurier, B. Mazeau, J.F. Millot, F. Molinié, J-P. Mols, J-P. Mouly, M. Mur, D. Neyret, T. Pédrol, S. Platchkov, G. Pontet, T. Pussieux, Y. Queinec , Ph. Rebourgeard, J. C. Sellier, G. Tarte, C. Veyssière, A. Zakarian,

DAPNIA CEA Saclay, 91191 Gif/Yvette Cedex, France

P. Bertin and A. Cosquer,

LPC/IN2P3, Clermont Ferrand, France

J. P. Chen and J. Mitchell,

Thomas Jefferson National Accelerator Facility, Newport News, VA 23606, USA

J-M. Mackowski and L. Pinard,

IPNL/IN2P3, Université Claude Bernard Lyon I, 69622 Villeurbanne cedex, France

Abstract

We built and commissioned a new type of Compton polarimeter to measure the electron beam polarization at the Thomas Jefferson National Accelerator Facility (Virginia, USA). The heart of this polarimeter is a High Finesse monolithic Fabry-Pérot cavity. Its purpose is to amplify a primary 300 mW laser beam in order to improve the signal to noise ratio of the polarimeter. It is the first time that a

High Finesse Fabry-Pérot cavity is enclosed in the vacuum of a particle accelerator to monitor the beam polarization by Compton polarimetry. The measured Finesse and amplification gain of the cavity are $F = 26000$ and $G = 7300$. The electron beam crosses this high power photon source at an angle of 23 mrad in the middle of the cavity where the photon beam power density is estimated to be 0.85 MW/cm^2. We have used this facility during the HAPPEX experiment (April-July 1999) and we give a preliminary measurement of Compton scattering asymmetry.

1 Introduction

A large fraction of the physics program at Jefferson Lab [1] uses polarized electrons of energy between 1 and 6 GeV at beam currents up to 100 μA. These experiments require a measurement of the electron beam polarization with an accuracy better than 3% and monitoring its ime-dependent variations. This can be achieved by using Compton scattering polarimetry which has been used elsewhere either at a higher current [2] or at a higher energy [3],[4]. This non-destructive method utilizes the detection of photons produced in Compton scattering of the electron beam off an intense circularly polarized photon beam.
For the experimental conditions of JLab, we designed a Compton polarimeter which uses a high Finesse Fabry-Pérot cavity as a high-power photon source [5]. In this paper, we report on the installation and commissioning of this polarimeter to measure the polarization of the electron beam delivered to experimental Hall A at JLab for the HAPPEX experiment [6],[7]. This is the first Fabry-Pérot cavity coupled to the beam pipe of an electron accelerator and used in a polarimeter to measure and monitor the polarization of an electron beam used for nuclear physics experiments.
The Compton scattering cross section has spin-dependent terms which results in an asymmetry A_{exp} in the rate of back-scattered photons. Measuring A_{exp} and the photon-beam polarization $\mathcal{P}_\gamma$, and knowing the longitudinal theoretical cross-section asymmetry A_l, the electron-beam longitudinal polarization $\mathcal{P}_e$ is derived from [5]: $A_{exp} = \mathcal{P}_e \mathcal{P}_\gamma A_l$.

We first describe the experimental set-up with a focus on the optical cavity. We then present the measured performance of the photon source and evidence of the Compton scattering signal. Finally, we give a preliminary analysis of data taken during the HAPPEX experiment at a beam energy of E=3.355 GeV and a beam current of $I_e = 40$ μA.

[1] Corresponding author. Tel.: +33 1 69083454; e-mail: adelbart@cea.fr

2 The JLab Hall A Compton Polarimeter

The polarimeter is described in figure 1. It was designed for the experimental Hall A at JLab and it can be operated for electron beam energies up to 8 GeV. The primary photon beam is delivered by a 300mW Continuous Wave Nd:Yag laser of energy $k = 1.165$ eV (λ=1064 nm). For this photon energy and an electron energy of 4 GeV, the back-scattered photons of energy greater than 40 MeV are emitted in a 350 μrad cone around the electron beam. We thus designed a 4-dipole magnetic chicane which deflects the electron beam and seperates it from the back-scattered photons to be detected. Polarized electrons scatter off circularly polarized photons stored and amplified in the Fabry-Pérot cavity which is enclosed in the lower beam pipe of the chicane, between the second and third dipoles. The crossing point, called the Compton Interaction Point (CIP), is thus located at the middle of the cavity.

The photon beam system is set on a vibration-isolated honeycomb table below the CIP and called the optics table. It is controlled and commanded from the Hall A counting room via the EPICS control system [8]. The photon beam system consists of :

- the optical setup which deals with transport, focusing and polarization shaping and measurement of the primary photon beam,
- the Fabry-Pérot cavity mechanics and optics,
- the opto-electronics system which locks the power build-up process for amplification.

The rate of back-scattered photons is measured in a $PbWO_4$ calorimeter. The electron beam helicity is reversed every 33 ms and the data acquisition system attributes the electron and photon beam parameters associated with each electron polarization state in order to compute the experimental asymmetry off-line. We also have the possibility to reverse the photon helicity in order to lower systematic errors. A silicon microstrip detector is currently being commissioned to measure the momentum of scattered electrons.
The output photon beam polarization $\mathcal{P}_\gamma^{out}$ is measured at the exit of the optical cavity. This measurement is used to determine the polarization $\mathcal{P}_\gamma$ of the amplified photon beam at the CIP.

This section is devoted to the magnetic chicane, the photon detector and the data acquisition system. The photon beam system is the subject of the next section.

2.1 The magnetic chicane and the associated vacuum system

The magnetic chicane consists of 4 identical dipoles (figure 2 and figure 2) which are controlled in series to return the electron beam to the Hall A experiment without altering its direction, energy and polarization. The vertical displacement of the electron beam in the central lower beam line can be varied to get and optimize the crossing of the electron and photon beams. This is achieved by slightly adjusting the field of the dipoles. The position of the beam is measured with downstream and upstream Beam Position Monitors (BPM). The background level is monitored with 4 Beam Diagnostics, each consisting of 4 scintillators read by PMTs.

Every part of the polarimeter beam line was optimized to ensure a low pressure and clean vacuum at the CIP. Cleanliness is required to keep the cavity mirrors free of any pollution which would lower the cavity build-up gain and therefore the Compton scattering luminosity.
Low pressure is needed to reduce as much as possible the Bremsstrahlung radiation seen by the photon detector. Because of the higher pressure in the beam pipe downstream of the polarimeter ($\approx 10^{-7}$ Torr), we use seven ionic pumps for an overall pumping capacity of 480 l/s. In order to minimize gas desorption, most components in contact with vacuum are stainless steel baked at 1000 ^{o}C during the manufacturing process. We also heat the chicane beam pipe at 180 ^{o}C for several hours after every vacuum break. A 10^{-8} Torr vacuum was thus obtained in the optical cavity.

2.2 Detection and acquistion of Compton scattering events

The scattered photons are detected and their energy is measured in a photon calorimeter made of 5x5 $PbWO_4$ scintillators. Each crystal is 20x20x230 mm^3 and is read out at one side by a Philips XP1911 photomultiplier tube. The crystals are enclosed in a 16 ^oC temperature controlled box because of the light yield sensitivity to temperature ($2\%/^oC$).
Lead tungstate crystal was chosen for its high density (8.28 g/cm^3), small Molière radius (2.19 cm), fast response (62% of the charge in 100 ns) and good radiation hardness. The calorimeter is thus compact with a minimum dead time. An energy resolution of $\frac{\sigma(E)}{E} = 1.76\% \oplus \frac{2.75\%}{\sqrt{E}} \oplus \frac{0.41\%}{E}$ was measured on the tagged photon beam line at the MAMI facility [9].

The data acquisition system of the Compton polarimeter was designed to collect the photon calorimeter signals at the expected 100 kHz rate with a dead time of less than 10%.
After amplification, the photomultipliers signals are used to generate a trigger

for the photon acquisition system, and these signals are integrated and measured by 10 fast ADC cards. To reach the desired counting rate, these ADCs are buffered and read out in blocks (10MB/s maximum data flux on VME bus). These values are then attributed to each electron beam polarization pulse (30.3 Hz rate), and some calculations, such as back-scattered photon energy histogramming, are processed on-line by two different PowerPC CPUs. In parallel, the electron and photon beam parameters are monitored at a frequency up to 600 Hz and attributed to each polarization pulse. These data are then stored in the same file on a Sun workstation.

3 The photon beam and its amplification by the High Finesse Fabry-Pérot cavity

The laser and all the optical components are aligned on three different breadboards for ease of maintenance procedures. These breadboards are mounted on the optics table (figure 3) which also supports the lower central beam pipe containing the optical cavity and the vacuum pumps and gauges. The control-command schematics of the system and the optical setup are shown in figures 4 and 5.
We chose a monolithic design for the Fabry-Pérot cavity. The following conditions are required to get and maintain the maximum power build-up :

- the stability parameter g must satisfy $-1 \leq g = 1 - \frac{L}{R} \leq 1$ where L is the cavity length and R is the radius of curvature of the mirrors,
- the two mirrors must be accurately aligned and oriented with respect to each other to avoid diffraction losses,
- the primary laser beam must be accurately injected into the cavity with the correct orientation and shape,
- the frequency of the primary laser has to be locked on a resonant frequency of the cavity.

For a monolithic cavity, the Pound-Drever locking technique [10] is well suited to mode-lock the laser frequency on a resonant frequency of the cavity. A first prototype of a low Finesse Fabry-Pérot cavity ($F = 1700$) has been described in our previous paper [11]. This prototype was mainly used to design and test an efficient and robust electronics for the Servo-loop control used for mode-locking [12]. The JLab Compton polarimeter uses the same primary laser (Lightwave [2] series 126) and the same opto-electronics mode-locking system which was improved to cope with the narrower bandwidth of the High Finesse cavity and the accelerator environment.

[2] Lightwave Electronics, 2400 Charleston Road, Mountain View CA 94043, USA

3.1.1 Description

To maximize the luminosity of Compton scattering, the photon beam size at the CIP has to be close to but greater than the electron Gaussian beam radius which is estimated around $\sigma_e \approx 70$ μm. This is achieved by mode-locking the Fabry-Pérot cavity on its fundamental mode which generates an amplified circular Gaussian beam whose smallest transverse dimension, called the waist, is located at the center of the cavity. The waist radius $\omega_{\gamma,0}$, measured at I_{max}/e^2, is given by $\omega_{\gamma,0}^2 = 4\sigma_{\gamma,0}^2 = \frac{\lambda L}{2\pi}\sqrt{\frac{1-g}{1+g}}$.

We chose to build a cavity of $g = -0.7$ with $R = 0.5$ m and $L = 0.85$ m whose waist radius is therefore $\sigma_{\gamma,0} = 123$ μm. This was a compromise between stability, ease of mode-locking, diffraction losses and mechanical setting up. The high-reflectivity cavity mirrors, M_{ce} and M_{cs}, are made of dielectric quarter-wave layers of alternate low-refractive index (SiO_2) and high-refractive index (Ta_2O_5) amorphous deposits on a super polished 10 mm diameter silica substrate. They were designed to have a transmittance of 137 ppm at $\lambda = 1064$ nm. We made and characterized 11 mirrors at the IN2P3/IPNL/SMA. We used the Double Ion beam Sputtering technique (or DIBS) to deposit the layers and we measured them in a class 1 clean room just after their fabrication. These mirrors have an average transmittance $T = 121 \pm 5$ ppm, an average diffusion $D = 6 \pm 2$ ppm and an average absorption $A < 2$ ppm. The two mirrors of the cavity are selected to have similar properties and we will assume they have the same transmittance T and the same total losses $A + D$.

For a monolithic Fabry-Pérot cavity the two high-reflectivity mirrors are placed on each side of a high-precision mechanical spacer. The relative position and orientation of the mirrors is fixed by the relative position and orientation of the two sides of the spacer. The spacer was designed to limit the mechanical vibrations of the structure and to facilitate pumping. This lead to the conical structure with oblong openings described in figure 3. The designed crossing angle of 23 mrad was chosen to ensure a 5 mm safety distance between the electron beam and the mirrors' edge. The specifications of the spacer are of the highest quality produced commercially, especially in terms of parallelism of the two faces of the spacer (≤ 300 μrad). A first prototype was successfully tested at Saclay. The final design is shown on figure 3. Both the prototype and the final cavity spacer were manufactured by the MECALIM company [3]. The mirrors of the cavity are mounted on the spacer in a Class 100 clean room and were kept protected from dust until the connection to the chicane beam

[3] MECALIM, zone industrielle de Beauregard, 19100 Brives, France.

pipe was completed.

3.1.2 Mode-locking

For Pound-Drever phase locking the frequency of the laser is modulated at 928 kHz by applying a sinusoidal voltage of 20 to 40 mV on the laser piezoelectric actuator which also provides the FAST control of the laser frequency. For larger detuning a Peltier module commands the Nd:YAG crystal's temperature for a SLOW frequency control. The detuning signal used by the feedback loop is then proportional to the phase of the laser beam reflected by the cavity.
The reflected beam is separated from the incident beam using a polarizing beamsplitter cube (figures 4 and 5). It is then collected by a Spectralon 2" integrating sphere S_r and the signal is read by a fast Si photodiode (PDR) which is mounted on an exit port of the sphere. This ensures a good collection of the reflected beam during coupling optimization. The sphere also acts as an equivalent optical density of 2 (intensity attenuation by a factor of 100) that makes the PDR operate in its linear regime.

The feedback electronics builds the detuning signal after a current-voltage conversion, filtering (Servo), demodulation and amplification of the PDR current [11,12]. To ensure loop stability, the three stages of the Servo controller have been adapted to the narrow bandwidth of the cavity ($\Delta\nu_{cav} = 6.8$ kHz). Both the search for a resonant frequency and the closing of the feedback loop are automatic. The mode-locking system is thus fully self-governing to react in a few seconds to an untimely unlock of the cavity or to automatically retrieve the build-up power after a photon beam shutdown or a photon beam polarization reversal (see section 3.3).

3.2 Optimizing the intra-cavity power

The maximum gain of a Fabry-Pérot cavity is $G_{max} = T/(A + D + T)^2$. The actual gain, and thus the actual power available for Compton scattering, is $G = \alpha_{00} G_{max}$ where α_{00} is the transverse fundamental mode coupling ratio and represents the amount of primary power actually amplified in the fundamental mode. We have an unavoidable coupling loss in the two modulation side bands used for Pound-Drever locking which was measured to be less than 2 % depending on the amount of modulation.
When mode-locked on its fundamental mode, the Fabry-Pérot cavity produces an amplified circular Gaussian beam of waist $\omega_{\gamma,0}$ along a path called the optical axis of the cavity. The optical axis passes through the two centers of curvature of the cavity mirrors and is imposed by the mechanical spacer. To

get α_{00} as high as possible, the injected primary photon beam must be as close as possible to the amplified photon beam in shape (same waist size and location at the middle of the cavity) and orientation (same path along the optical axis).

3.2.1 Injected photon beam shape coupling

The laser delivers an elliptical Gaussian beam whose dimensions have been measured by a beam-sampling technique using a dual-slits scan head from Photon inc.[4] with a 10 μm precision. The beam dimensions at 500 mm from the laser head are $\omega_x = 680$ μm and $\omega_y = 870$ μm, respectively in the horizontal and vertical plane. A first anti-reflective coated convergent lens L_1 with a focal length of $f_1 = 400$ mm is used to get a collimated beam of size $\omega_x = 605$ μm by $\omega_y = 825$ μm at the quarter-wave plate location. This will permit the future use of a Pockels Cell in order to reverse the photon beam polarization faster (up to 100 kHz) than with a quarter-wave plate.

In order for the incident beam to have the same shape as the mode-locked fundamental mode, the incident beam must have the same waist size $\omega_{\gamma,0}$ at the middle of the cavity located 2.905 m from the laser exit. This can be done by a telescope composed of two AR coated lenses L_2 and L_3. The focal lengths and locations of the lenses are determined by Gaussian beam calculations. These calculations must account for the equivalent focal length $f_4 = -1.087$ m of the spherical entrance cavity mirror. The choice of a solution is guided by the focal lengths commercially available and the space available between the quarter-wave plate and the first remote-controlled mirror M_1. This leads to the use of a divergent lens L_2 with focal length $f_2 = -50$ mm and a convergent lens L_3 with focal length $f_3 = 200$ mm (figure 5).

The theoretical beam size is shown on figure 6. At the CIP, the experimental checking is not possible with our scan head because of the very low power transmitted through the entrance cavity mirror (~ 30 μW). This is the reason why the position of the lenses was tuned before the cavity was placed. Without the entrance cavity mirror, we manage to focuse the beam 11 cm upstream of the CIP with a measured beam size of $\omega_x = 205$ μm by $\omega_y = 150$ μm. This is in good agreement with Gaussian beam calculations (figure 6a). After passing through the entrance cavity mirror, the beam is theoretically focused at the CIP with dimensions of $\omega_x = 210$ μm and $\omega_y = 285$ μm (figure 6b). An unavoidable 3 % coupling loss is predicted because of the beam ellipticity. With the cavity mode-locked, the position of lens L_3 can be fine-tuned by remote control to maximize the intra-cavity power. A correction of less than 0.5 mm is usually necessary.

[4] Photon Inc., 6860 Santa Teresa Blvd., San Jose, CA 95119-1205, USA.

3.2.2 Injected photon beam orientation coupling

When mode-locked on its fundamental mode, the Fabry-Pérot cavity generates an amplified Gaussian beam which is aligned on the optical axis of the cavity. A periscope made of two remote controlled steering mirrors M_1 and M_2 (see figure 4) is used to accurately align the primary photon beam with respect to the optical axis of the cavity with a measured angular resolution of 10 μrad.

Without the cavity between the input and output stands (figure 3), the beam was first accurately aligned on the middle of the 12.5 mm diameter steering mirrors M_e and M_s with the help of two 4 cell photodiodes placed in transmission of the mirrors. The Fabry-Pérot cavity was then inserted and the beam pipe closed. The incident and reflected photon beams are made coincident on the mirror M_{r2} seen by a CCD camera with the help of the periscope. At this stage, we usually observe high-order transverse modes and a weak fundamental mode. With the incident beam mode-locked on this weak fundamental mode, we finally get the maximum intra-cavity power by slightly adjusting the incident beam (< 100 μrad) until the output power measured by the integrating spheres S_1 and S_2 is maximized. This procedure is fully automated. We routinely get a coupling ratio α_{00} close to the theoretical limit of 95 %.

3.3 Photon beam polarization

3.3.1 Polarization shaping and transport to CIP

A Faraday Isolator with a measured isolation of 36 dB protects the laser from reflected light. The 1/300 linear polarization of the laser beam is first purified (up to 1/100 000) by the output polarizer of the isolator. It is then rotated with a half-wave plate to be perfectly aligned with the direction of transmission of the laser polarizing beamsplitter (chosen vertical). It is eventually transformed to circular polarization with a remote controlled quarter-wave plate. The fast axis of the quarter-wave plate can be carefully oriented to obtain the best right-handed or left-handed polarization at the CIP.

Two pairs of identical dielectric mirrors whose plane of incidence are orthogonal within 1^o (M_1 - M_{r2} and M_2 - M_e) propagate the circular polarization with minimal distortion. With this compensated scheme, we managed to get a 99.7 % left-handed and a 99.6 % right-handed polarization at the entrance of the cavity (M_e exit). This has been obtained for an angle between the linear vertical input polarization and the fast axis of the quarter-wave plate of respectively 50^o counterclockwise and 51^o clockwise.

3.3.2 On-line output polarization measurement

The photon beam polarization is measured on-line at the exit of the cavity after the pair of compensated mirrors M_s - M_3. A Harmonic Beam Sampler (HBS) is used to diffract the beam at 10^o into two first-order diffracted beams, each one containing 1 % of the incident beam. A CCD camera and a fast Hamamatsu Si photodiode are placed on the path of these two diffracted beams. The first one allows to view the amplified beam shape and the second one is used for decay time measurements (see section 3.4). The central transmitted beam carries 97.4 % of the incident power and its polarization is preserved within 0.1 %. This polarization $\mathcal{P}_\gamma^{out}$ is eventually measured by the combination of a Wollaston Calcite prism and a quarter-wave plate whose fast axis is accurately oriented at 45^o with respect to an optical axis of the prism. $\mathcal{P}_\gamma^{out}$ is the Degree Of Circular Polarization (DOCP) of the photon beam which is measured by the fourth normalized Stokes parameter S_3 [13]. S_3 is positive for a left-handed helicity and negative for a right-handed helicity. Using the Stokes formalism, one can show that $\mathcal{P}_\gamma^{out}$ is linked to the two calibrated beam powers $\mathbf{P}_{S_1}$ and $\mathbf{P}_{S_2}$ transmitted through the Wollaston prism by $\mathcal{P}_\gamma^{out} = S_3 = \frac{\mathbf{P}_{S_2} - \mathbf{P}_{S_1}}{\mathbf{P}_{S_2} + \mathbf{P}_{S_1}}$.

To measure $\mathbf{P}_{S_1}$ and $\mathbf{P}_{S_2}$ we use an InGaAs photodiode placed at an exit port of a 2" Spectralon integrating sphere (Labsphere Inc.[5]). The photodiodes have been calibrated by the manufacturer (Micro-Controle company [6]) and a powermeter reads the scattered flux $\mathbf{P}_{m_2}$ and $\mathbf{P}_{m_1}$ seen by the photodiodes. We have calibrated the overall response of the two Sphere + photodiode systems with a calibrated powermeter from Coherent Inc.[7] Their response is linear up to 700 mW incident power with a calibration coefficient K_{S_i} given by $\mathbf{P}_{S_i}[mW] = K_{S_i}.\mathbf{P}_{m_i}[\mu W]$ (Table 1).

The quarter-wave plate is motorized and we can derive the 4 Stokes parameters of the photon beam from the measurements of $\mathbf{P}_{S_1}$ and $\mathbf{P}_{S_2}$ for at least three different orientations of the fast axis. This complete characterization of the slightly elliptical polarization (orientation and DOCP) will be necessary to obtain the absolute photon beam polarization at the CIP.

3.4 Performance of the Fabry-Pérot cavity

The intra-cavity power is given by $\mathbf{P}_{cav} = \alpha_{00} G_{max} \mathbf{P}_i = \mathbf{P}_t / T$ where $\mathbf{P}_i$ (resp. $\mathbf{P}_t$) is the injected power at the entrance of the cavity (resp. the power at the exit of the cavity). The injected power $\mathbf{P}_i$ is deduced from the power measurements $\mathbf{P}_{S_e}$ in transmission of the mirror M_1 (integrating Sphere S_e +

[5] Labsphere inc., North Sutton, NH 03260, USA.
[6] Micro-Controle, P.A. Saint Gunault - BP 189, 91006 Evry cedex, France.
[7] Coherent Inc., 5100 Patrick henry Drive, Santa Clara CA 95054, USA.

photodiode) with $\mathbf{P}_i[mW] = K_e.\mathbf{P}_{S_e}[\mu W]$. The output cavity power $\mathbf{P}_t$ is deduced from the power measurements P_{S_1} and P_{S_2} by $\mathbf{P}_t[mW] = K_t.(\mathbf{P}_{S_1}[mW] + \mathbf{P}_{S_2}[mW])$. The calibration coefficients K_e and K_t have been determined for the two circular polarizations and are given in Table 1.

Although the loss ratio $\beta = \frac{A+D}{T}$ of the mirrors has been measured at the IN2P3/IPNL/SMA ($\beta \approx 0.058$), we regularly measure it in case of mirror pollution during the installation of the cavity. We also need to monitor it on-line to detect a possible damaging of the mirrors (pollution or radiation damage).

Neglecting the power carried by the modulation side bands, one can show that α_{00} and β can be derived from the following equations :

$$\beta = \frac{1}{2}\left(\frac{\mathbf{P}_i}{\mathbf{P}_t}\left(1 - \frac{\mathbf{P}_r^{cL}}{\mathbf{P}_r^{oL}}\right) - 1\right) \tag{1}$$

$$\alpha_{00} = \frac{\mathbf{P}_t}{\mathbf{P}_i}(1+\beta)^2 \tag{2}$$

where $\mathbf{P}_r^{cL}$ and $\mathbf{P}_r^{oL}$ are the powers reflected by the cavity with the feedback loop respectively closed and opened. The ratio $\mathbf{P}_r^{cL}/\mathbf{P}_r^{oL}$ is measured on line by the ratio $V_{PDR}^{cL}/P_{PDR}^{oL}$ where V_{PDR}^{cL} and V_{PDR}^{oL} are the PDR voltages (corrected from background signal) measured with closed and opened loop respectively.

Finally, for a High-Finesse cavity ($F > 10000$), the Finesse is linked to the total losses and transmittance of the mirrors by $A + D + T = \pi/F = L/(c.T_d)$ where T_d is the decay time of the cavity. With the cavity mode-locked on its fundamental mode, we measure the experimental cavity decay time by shutting off the diode pumping of the laser (Standby mode) and recording the PDR or PDT voltage on a fast digital oscilloscope. T_d is obtained by fitting the convolution of the theoretical exponential of the emptying of the cavity by the experimental exponential decay of the laser itself (decay time ≈ 6 μs).

The results are summarized in Table 2. The performance of the system is similar for the two circular polarizations. An average of 92.5 % of the 229 mW of injected power is coupled in the fundamental mode of the cavity. The intra-cavity power is close to 1.6 kW, i.e. 0.85 MW/cm^2 power density at the CIP. The power density on the cavity mirrors is 125 kW/cm^2 which is below their predicted damage limit (≤ 1 MW/cm^2 for a continuous wave). An example of recording of the intra-cavity power with a 10 μA electron beam crossing (figure 7) shows a 3 % stability over 10 hours.

We are currently working on the absolute calibration of the photon beam polarization $\mathcal{P}_\gamma$ at the CIP. The difficulty comes from the inherent impossibility to perform a measurement at the CIP because of the power buildup

process and from the non-accessibility for on-line optical measurements inside the central vacuum beam pipe. For the time being, the polarization measurements with and without the cavity are given in Table 2. The measured output polarization $\mathcal{P}_\gamma^{out}$ is stable at 0.05 % (figure 7).

4 Preliminary analysis of Compton events

This chapter is dedicated to a preliminary analysis of the Compton events acquired with the complete polarimeter setup. The photon beam settings are those previously presented (Table 2). The electron beam conditions are those of the HAPPEX experiment, E=3.355 GeV and $I_e = 40$ μA, unless otherwise specified. We finally derive an experimental longitudinal integrated asymmetry which is the first step towards an electron beam polarization measurement.

4.1 Background back-scattered rate in the photon detector

Background is measured with the cavity turned off.The Background counting rate in the photon detector is mainly due to bremsstrahlung radiation emitted by electrons when they interact with residual gas or with matter. The low pressure vacuum (10^{-8} Torr) obtained in the cavity (section 2.1) is the first step to minimize the background rate. The second step is to carefully center and focus the electron beam in the polarimeter chicane and in the upstream accelerator beam pipe. This tuning is demanding because the electrons must go through the small apertures ($\pm$5 mm) located on each side of the mechanical spacer of the cavity (figure 3).
After a necessary training period, we were able to routinely lower the overall background counting rate in the central crystal of the photon detector below $0.25 kHz/\mu$A for the 3.355 GeV electron beam of HAPPEX. The lowest background rate obtained was $0.1 kHz/\mu$A. An example of a raw background energy spectrum is shown in figure 8.

4.2 Beam Crossing and raw energy spectrum of back-scattered photons

Once the background counting rate has been lowered to an acceptable value, the electron beam is moved vertically (section 2.1) until it crosses the photon beam inside the cavity. Figure 9 displays the counting rate in the central crystal during the scanning procedure. It corresponds to the expected luminosity

of the two interacting beams :

$$L_{max}(y) = \frac{1}{\sqrt{2\pi}} \frac{I_e}{e} \frac{P_L \lambda}{hc^2} \frac{G}{\sqrt{\sigma_e^2 + \sigma_\gamma^2}} \frac{(1 + cos\alpha_c)}{sin\alpha_c} \exp\left(-\frac{y^2}{2(\sigma_e^2 + \sigma_\gamma^2)}\right) \qquad (3)$$

where y is the vertical distance between the two beams, I_e is the electron beam intensity, P_L is the intra-cavity power, λ is the laser wavelength, G is the amplification gain of the optical cavity, σ_e and σ_γ are electron and photon beam sizes at the CIP, and α_c is the crossing angle of the two beams. The photon beam size defined by the cavity is $\sigma_{\gamma,0} = 123\ \mu m$ at the CIP. Using equation 3, we found the electron beam size to be $\sigma_e \approx 75\ \mu m$, which is consistent with the accelerator specifications ($\sigma_e \approx 100\ \mu m$).

The final magnet settings were determined by the maximum luminosity of the position scan. The counting rate variations correlated to the cavity laser power are shown in figure 10, as the locking system was turned on and off. We observed an excess of $1.5 kHz/\mu A$ in the counting rate when the cavity is mode-locked. During the HAPPEX experiment, the signal over background ratio was better than 3, with a maximum of 20.
To construct the Compton energy spectrum, the background has to be subtracted. The ADC spectrum obtained with background events is substracted from the raw spectrum when the cavity is on. The two spectra are normalized in the high energy region where no Compton scattering is expected and where the spectra have the same shape. Figure 8 shows an example of the raw energy spectrum of back-scattered photons.

4.3 Experimental asymmetry

Using the total rate in the central crystal of the photon detector, one can construct a pulse-by-pulse asymmetry from the two opposite electron beam helicity states. The rate is normalized to the beam intensity and the asymmetry is corrected for the dilution due to the background. Figure 11 shows the pulse by pulse asymmetry distributions for the two photon polarization states, A_{right} and A_{left}. The average result is $A_{right} = -1.14 \pm 0.02$ % and $A_{left} = 1.18 \pm 0.02$ %. A statistical accuracy of 1 % is achieved within one hour. As expected, the experimental asymmetry flips sign with the photon helicity.

To extract the electron beam polarization, the experimental asymmetry has to be compared to the theoretical cross-section asymmetry $< A_l >$ in the corresponding energy range. Determination of the beam polarization is sensitive to :

- the energy threshold E_0 above which photons are detected in the calorimeter in order to compute $< A_l >$ given by :

$$< A_l >= \frac{\int_{E_0}^{\infty} A_l(E) \frac{d\sigma}{dE} dE}{\int_{E_0}^{\infty} \frac{d\sigma}{dE} dE},$$

- the energy calibration and resolution of the detector,
- false asymmetries due to the helicity-correlated beam parameters, such as position, angle and shape.

5 Conclusion

We have successfully designed and operated a new kind of Compton polarimeter at JLab which uses a High Finesse Fabry-Pérot cavity as a high power photon source. A 300 mW Continuous Wave laser beam is amplified by a factor of 7300 to provide a 1.6 kW photon beam which crosses the electron beam at an angle of 23 mrad. It was used for four months during the HAPPEX experiment [7] with no noticeable degradation of its performance. This is a remarkable result since the Fabry-Pérot cavity mirrors are placed at 5 mm from the electron beam.

A preliminary analysis of the Compton scattering events aquired during the first two months of operation is very encouraging. Signal to noise ratio in the photon detector is around 10 and analysis of the data leads to an experimental cross-section asymmetry of $|A_{exp}| = 1.16 \pm 0.2$ %. The next step towards the electron beam polarization measurement is the study of systematic errors, primarily due to the calibration and resolution of the photon calorimeter, the false asymmetries due to helicity correlated beam parameters, and the absolute calibration of the photon beam polarization at the CIP. The analysis is under way and we expect to monitor the relative variations of the electron beam polarization with a 2% uncertainty and its absolute determination with a 3% uncertainty.

6 Acknowledgments

We would like to thank the technical staffs of IN2P3 and TJNAF for their contributions. We are grateful to J. Feltesse and C. W. de Jager for their constant support.

References

[1] L. Cardman, Nuclear Physics News, Vol.6, No. 4 (1996) 18.

[2] I. Passchier et al., Nucl. Instr. and Meth. A414 (1998) 446.

[3] M.Woods et al., Proc. SPIN96 Conference, World Scientific, Singapore, 1996, p. 843.

[4] D. P. Barber et al., Nucl. Instr. and Meth. A329 (1993) 79.

[5] G. Bardin et al., "Conceptual Design Report of a Compton Polarimeter for CEBAF Hall A", Internal Report DAPNIA-SphN-96-14 (1996).

[6] HAPPEX Collaboration, Phys. Rev. Lett. 82 (1999) 1096.

[7] HAPPEX Collaboration, to be submitted to Phys. Rev. Lett.

[8] EPICS, Experimental Physics and Industrial Control Systems. Web site : http://www.aps.anl.gov/xfd/SoftDist/Welcome.html.

[9] D. Neyret et al., "A photon calorimeter using lead tungstate crystals for the Cebaf hall A Compton polarimeter", Nucl. Instr. and Meth. A443 (2000) ?.

[10] R. W. P. Drever et al., Appl. Phys. B 31 (1983) 97.

[11] J.P. Jorda et al., Nucl. Instr. and Meth. A412 (1998) 1.

[12] J.P. Jorda, "Mise au point d'une cavité Fabry-Pérot pour la polarimétrie Compton", thèse de doctorat de l'université Paris 6, soutenue le 31 octobre 1997.

[13] S. Huard, "Polarisation de la lumière", Masson (1993).

List of Tables

List of Figures

Calibration Coefficient	**Left polarization**	**Right polarization**
$K_{S_1}[mW/\mu W]$	0.238 ± 0.002	0.238 ± 0.002
$K_{S_2}[mW/\mu W]$	0.268 ± 0.002	0.268 ± 0.002
$K_e[mW/\mu W]$	236 ± 3	244 ± 3
K_t	1.162 ± 0.002	1.152 ± 0.002

Table 1
Calibration coefficients for the photon beam power measurements.

	Left polarization	**Right polarization**
Cavity length [m]	0.85 ± 10^{-4}	0.85 ± 10^{-4}
Vacuum [Torr]	$\simeq 10^{-8}$	$\simeq 10^{-8}$
Injected power $\mathbf{P}_i$ [mW]	229 ± 3	229 ± 3
Modulation amplitude [mV]	10	10
PDR signal with opened loop [mV]	874 ± 8	878 ± 8
PDR signal with closed loop [mV]	118 ± 8	107 ± 10
PDR background signal [mV]	36.4 ± 0.5	36.4 ± 0.5
Coupling ratio $\alpha_{00} = \frac{P_t}{P_i}(1+\beta)^2$	0.918 ± 0.012	0.930 ± 0.014
Loss ratio $\beta = \frac{A+D}{T}$	0.149 ± 0.013	0.138 ± 0.013
Cavity decay time T_d $[\mu s]$	23.5 ± 0.5	23.5 ± 0.5
Cavity Finesse $F = \pi \frac{T_d c}{L}$	26040 ± 550	26040 ± 550
Cavity bandwidth $\Delta\nu_c = \frac{FSR}{F}$ [kHz]	6.8 ± 0.14	6.8 ± 0.14
Mirror transmittance T [ppm]	105 ± 2.5	106 ± 4
Mirror total losses $A + D$ [ppm]	16 ± 1	15 ± 1
Cavity maximum gain $G_{max} = \frac{T}{(A+D+T)^2}$	7210 ± 200	7290 ± 200
Output powers		
$\mathbf{P}_{s1}$ [mW]	0.646 ± 0.003	142.1 ± 0.4
$\mathbf{P}_{s2}$ [mW]	136.2 ± 0.4	1.031 ± 0.004
Injected polarization $\mathcal{P}_\gamma^{injected}$ without cavity	0.997 ± 0.005	-0.996 ± 0.005
Output polarization $\mathcal{P}_\gamma^{out}$ without cavity	0.989 ± 0.005	-0.993 ± 0.005
Output polarization $\mathcal{P}_\gamma^{out}$ with cavity	0.991 ± 0.005	-0.986 ± 0.005
Cavity output power $\mathbf{P}_t$ [mW]	159.0 ± 1.5	165 ± 1
Intra-cavity power $\mathbf{P}_{cav} = \frac{\mathbf{P}_t}{T}$ [W]	1515 ± 50	1550 ± 50
Intra-cavity power $\mathbf{P}_{cav} = \alpha_{00} G_{max} \mathbf{P}_i$ [W]	1545 ± 50	1580 ± 50
Estimated intra-cavity power $\mathbf{P}_{cav}$ [W]	1530 ± 50	1565 ± 50

Table 2
Main features of the Fabry-Pérot cavity (measured with electron beam crossing)

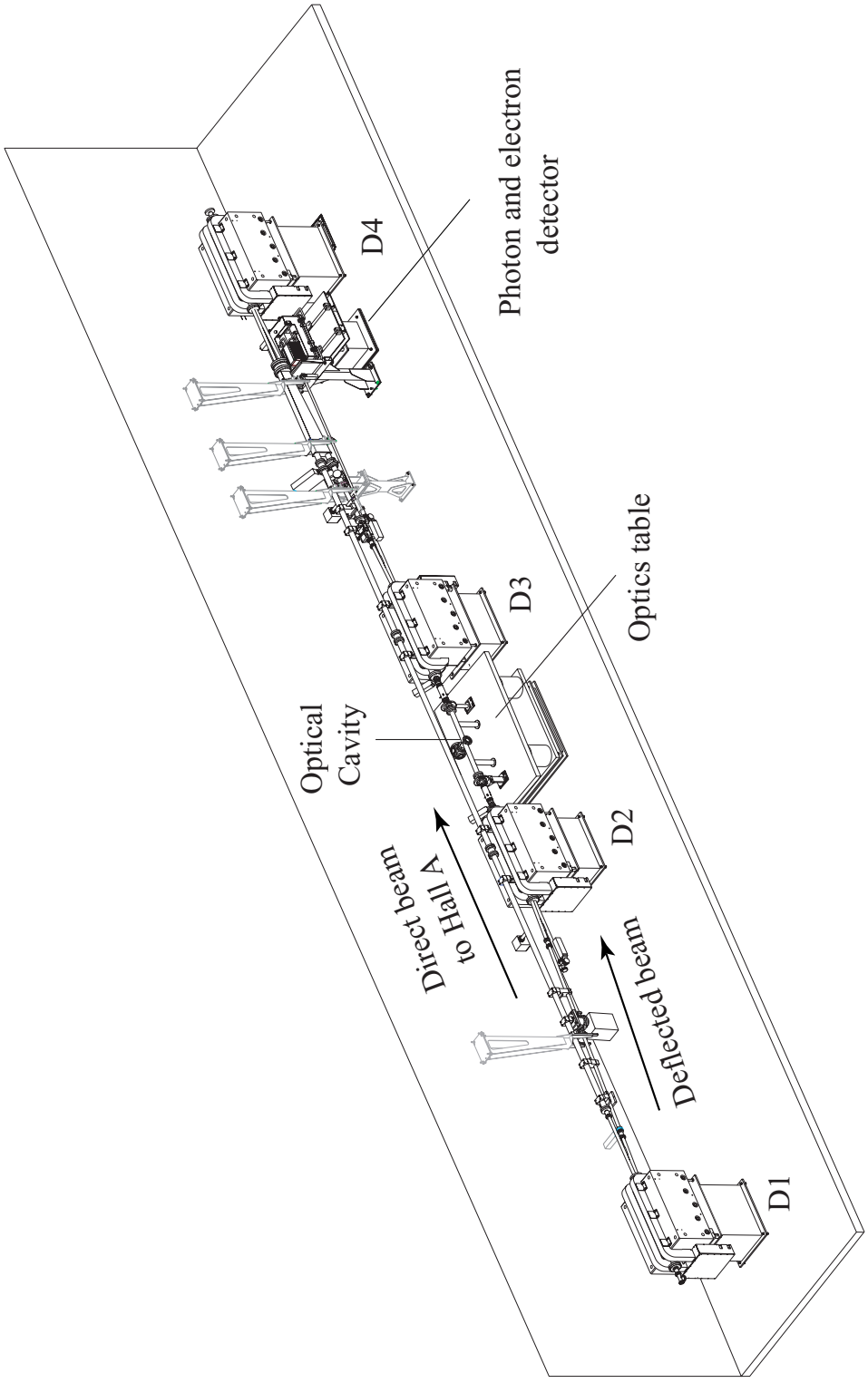

Fig. 1. *3D view of the TJNAF Hall A Compton Polarimeter.*

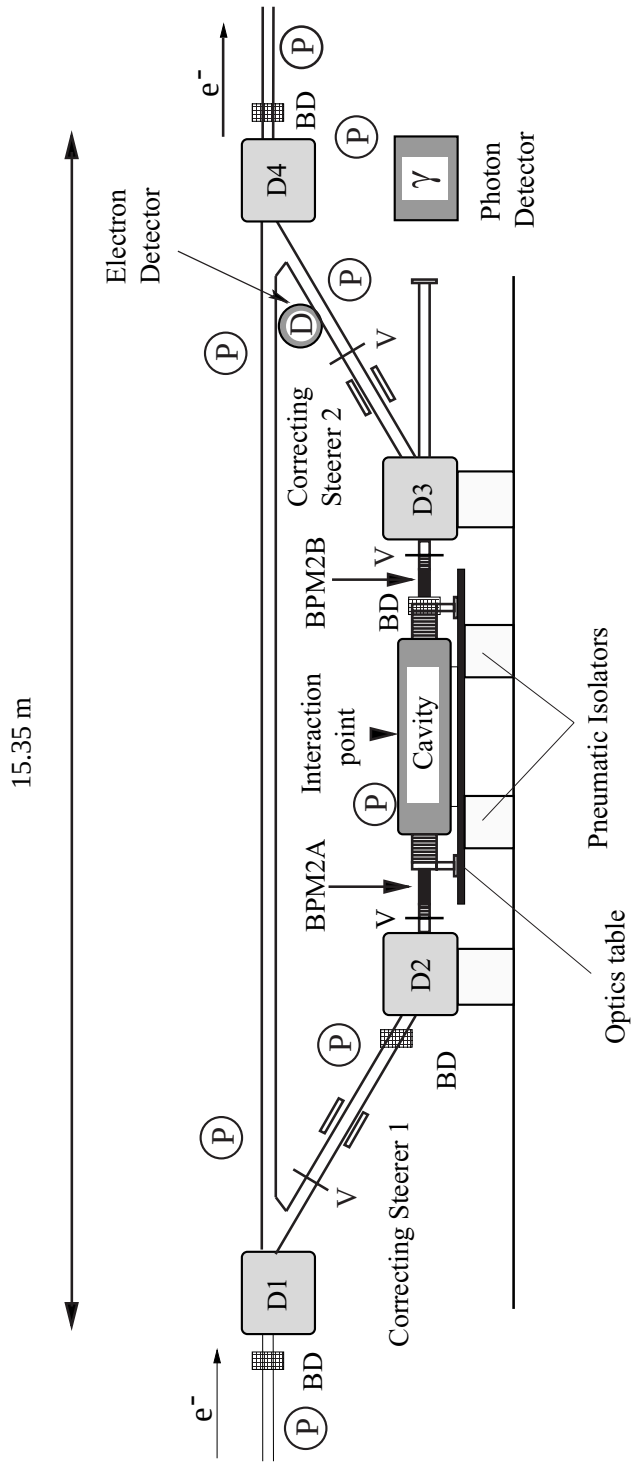

Fig. 2. *Detailed side view of the TJNAF Hall A Compton Polarimeter. P : ion pumps, BD : beam diagnostics, V : pneumatic vacuum valves.*

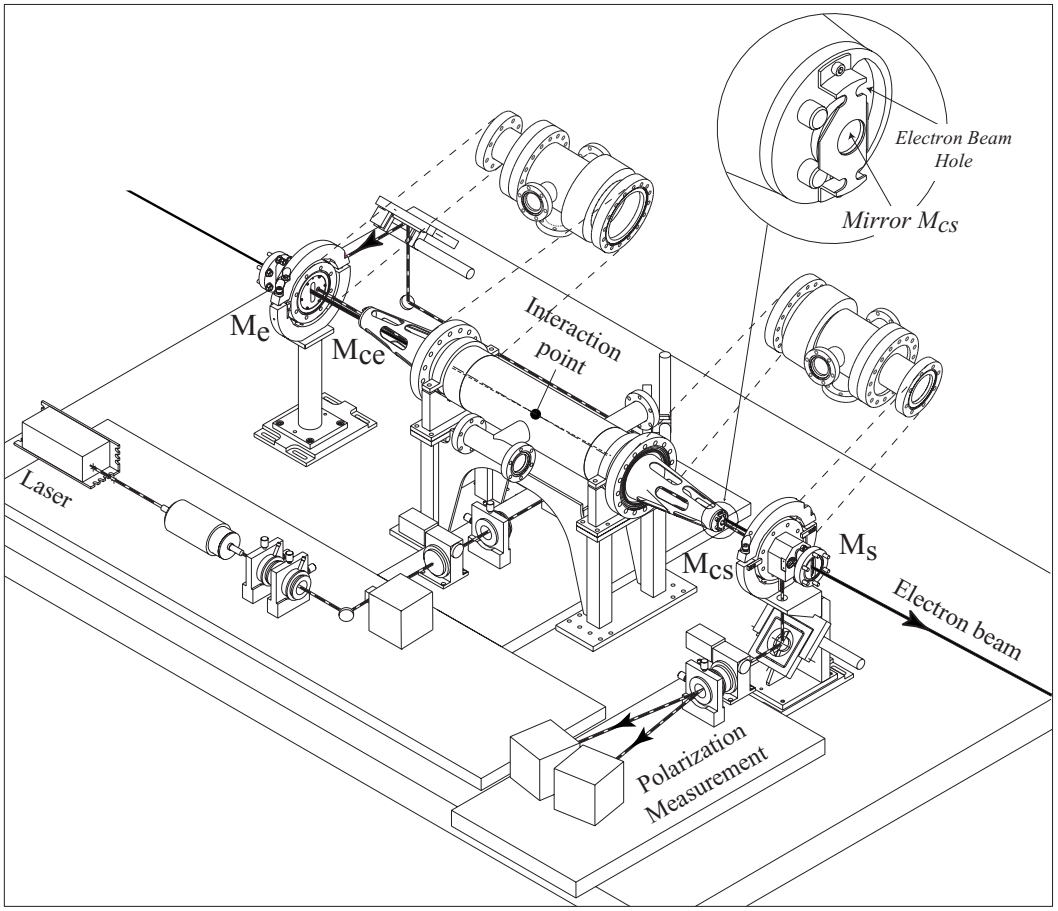

Fig. 3. *3D view of the optics table with the monolithic cavity (beam pipe opened).*

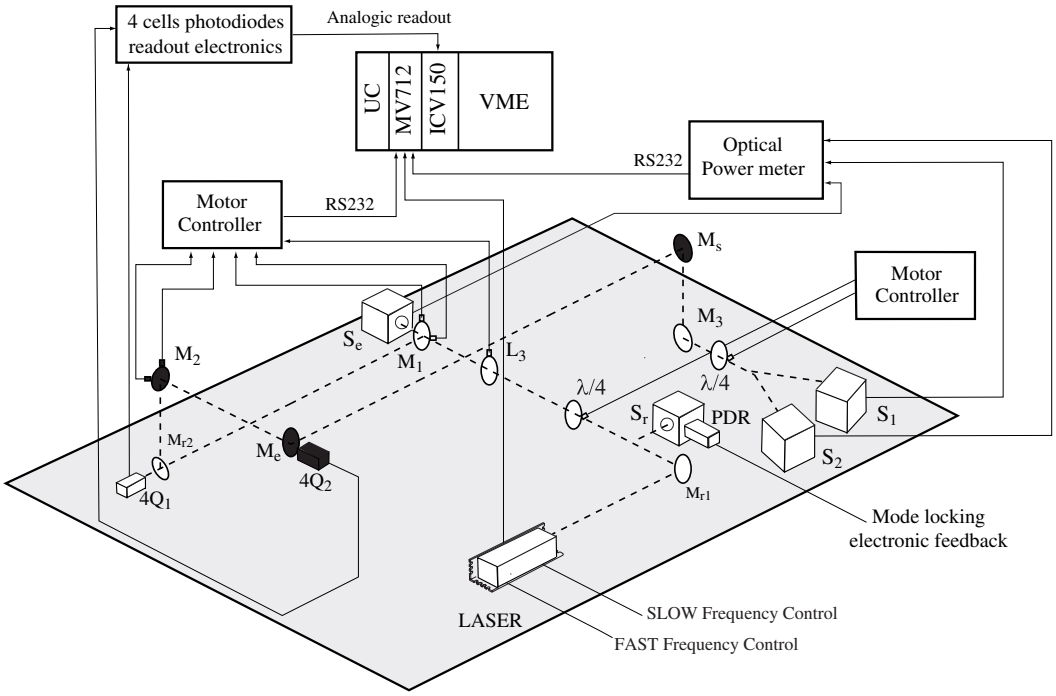

Fig. 4. *Functional view of the Fabry-Pérot cavity system.*

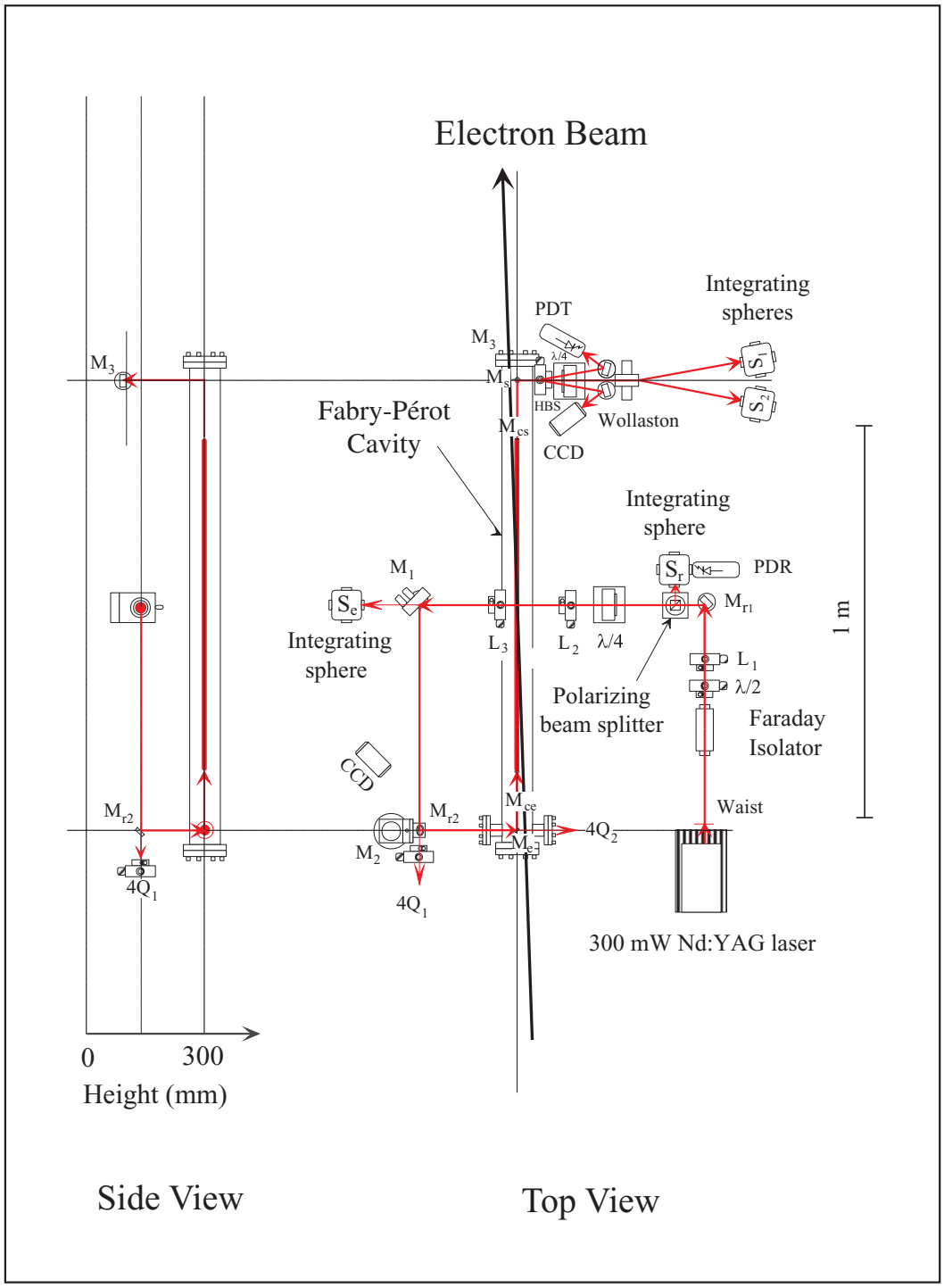

Fig. 5. *Layout of the optics table in the hall A tunnel (top and side views).*

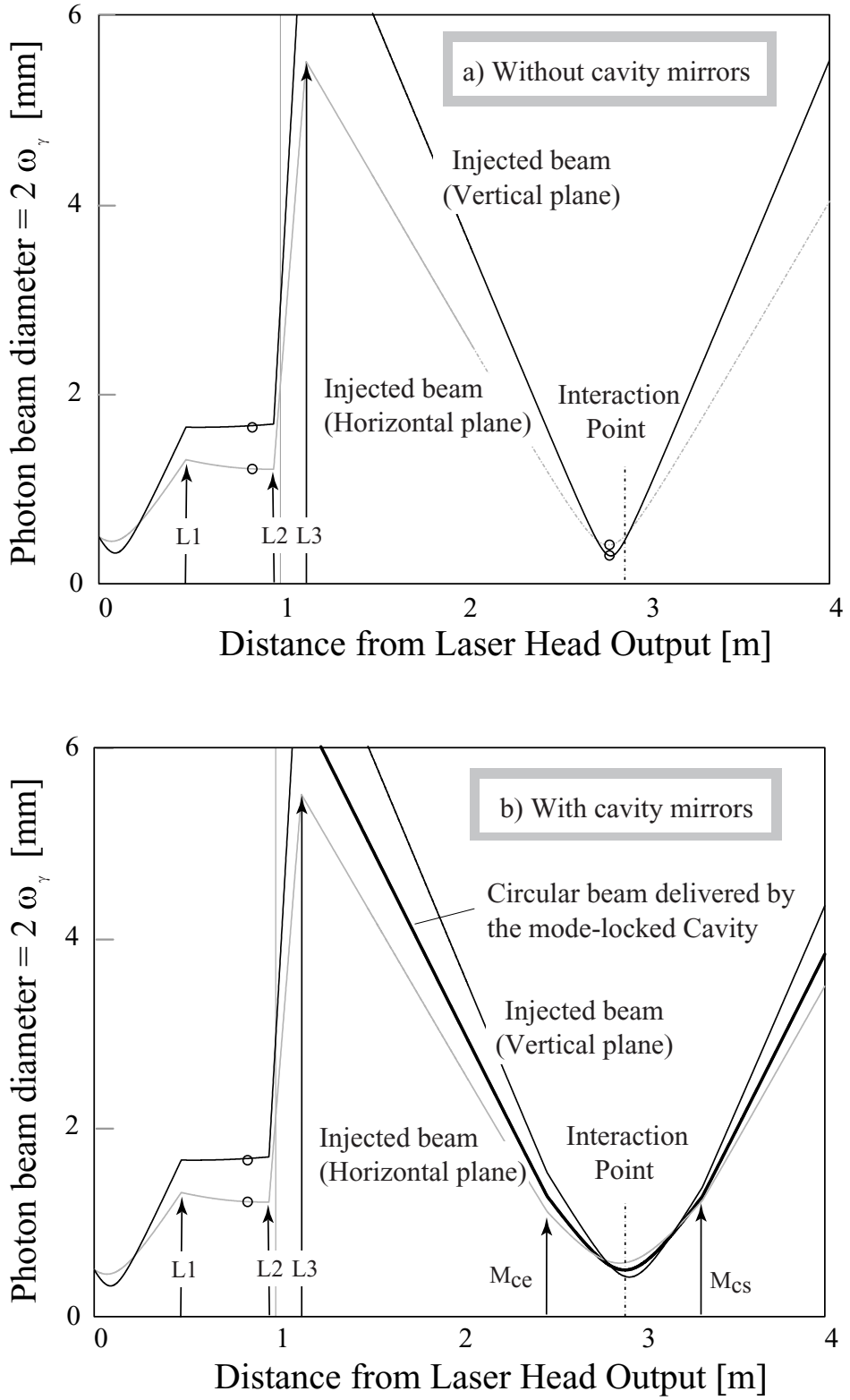

Fig. 6. *Calculated and measured photon beam diameter ω_γ as a function of the distance along the beam path from the laser head output. The black (resp. gray) curves correspond to the vertical (resp. horizontal) plane in the cavity. The circles represent the beam diameter measured with the dual-slits scan head.*

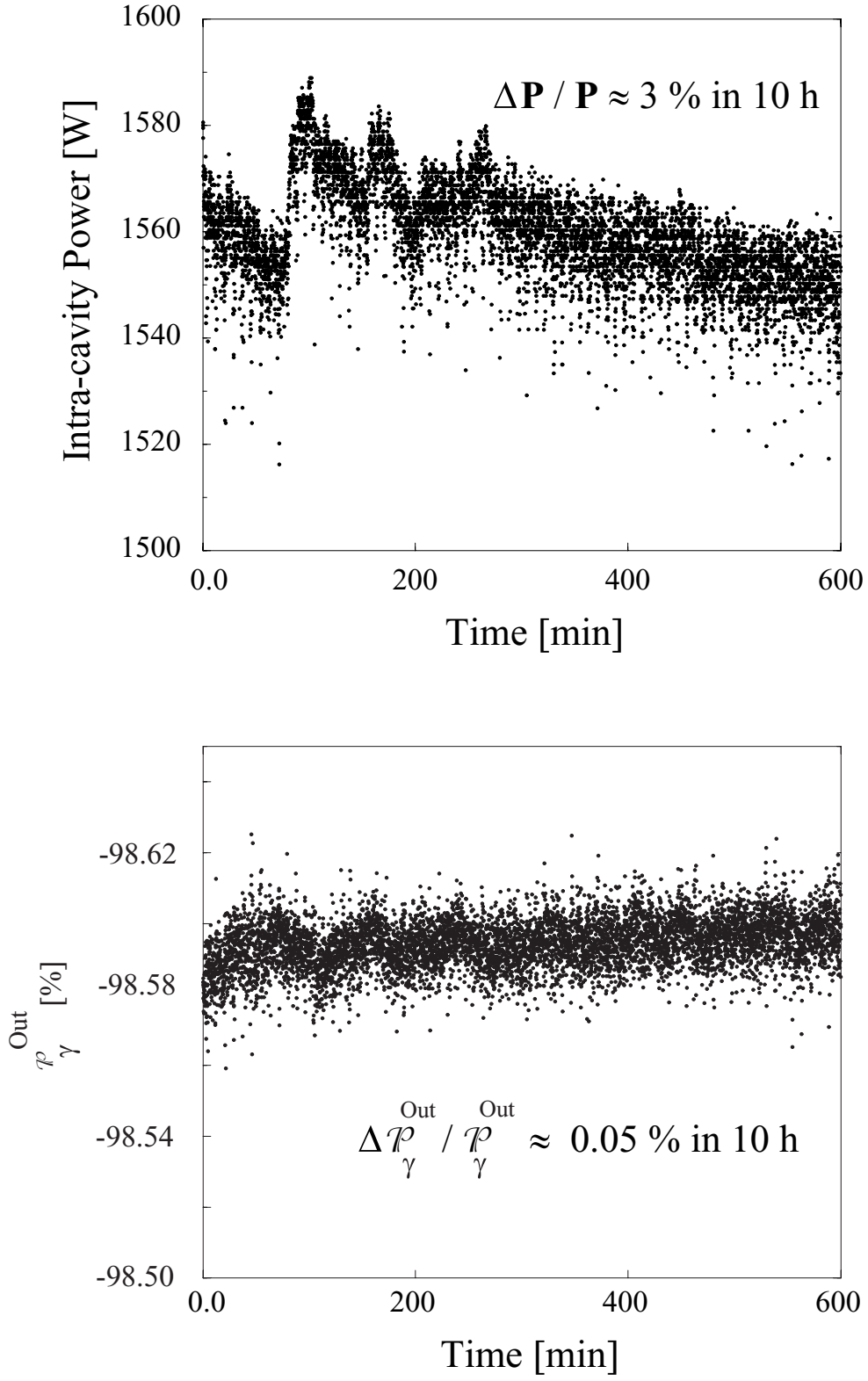

Fig. 7. *Intra-cavity power (top) and output photon beam polarization (bottom) over a 10 hours period with a 10 μA electron beam.*

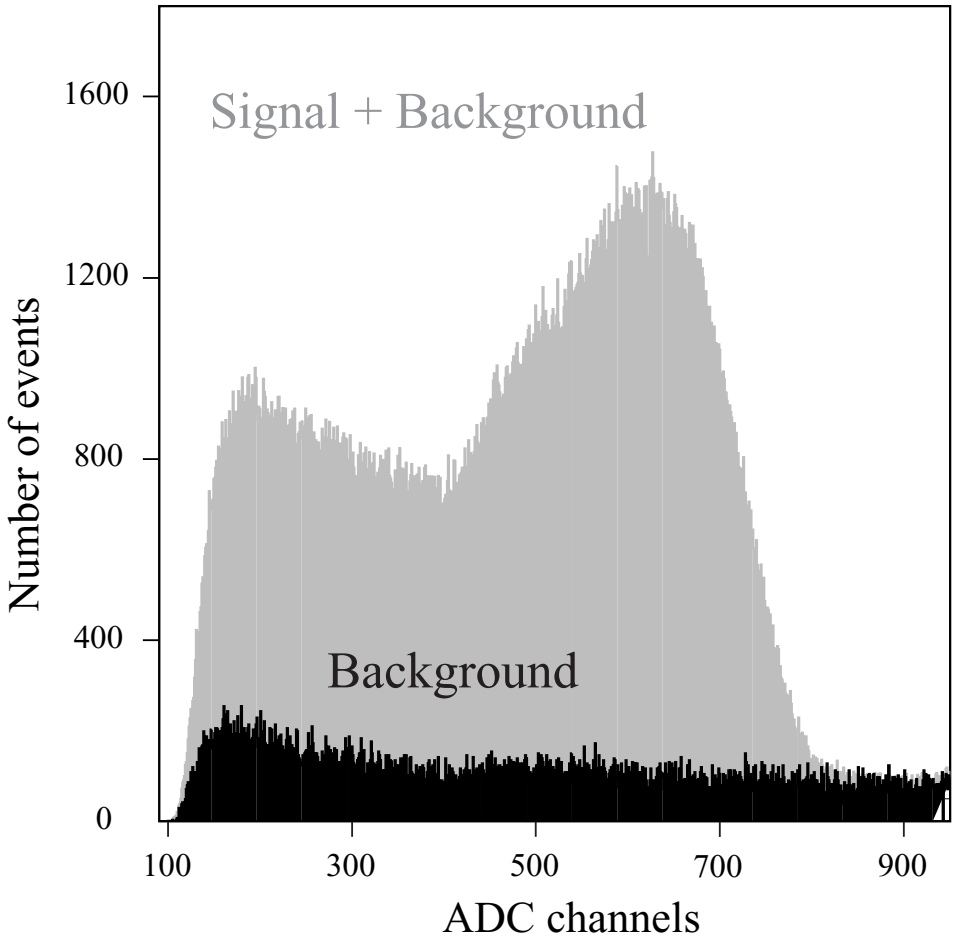

Fig. 8. *Background substraction : normalized Signal + Background and Background spectra. The Compton edge is around ADC channel 500 corresponding to an energy of about 190 MeV of the backscattered photon.*

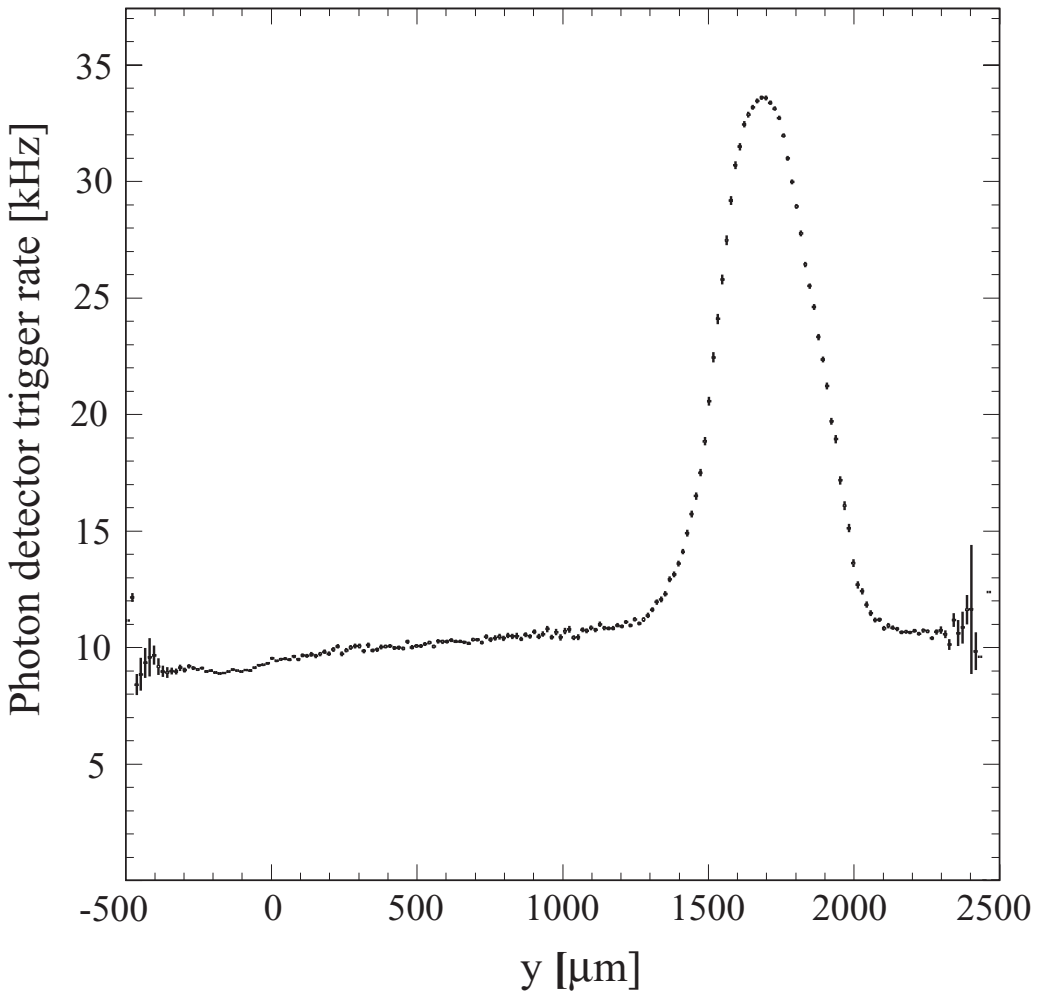

Fig. 9. *Rate in the central crystal of the photon detector as a function of the vertical position y of the electron beam. The electron beam current was* 10 μA.

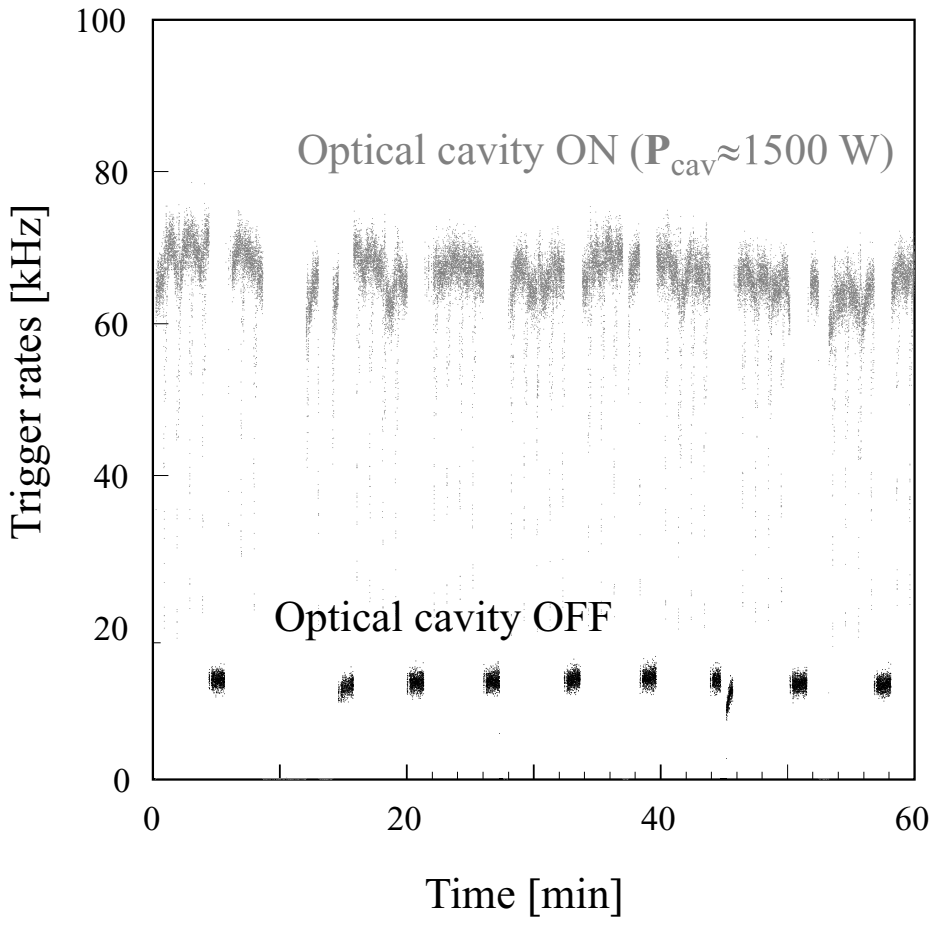

Fig. 10. *Correlation between the measured counting rates in the photon detector and the intra-cavity power.*

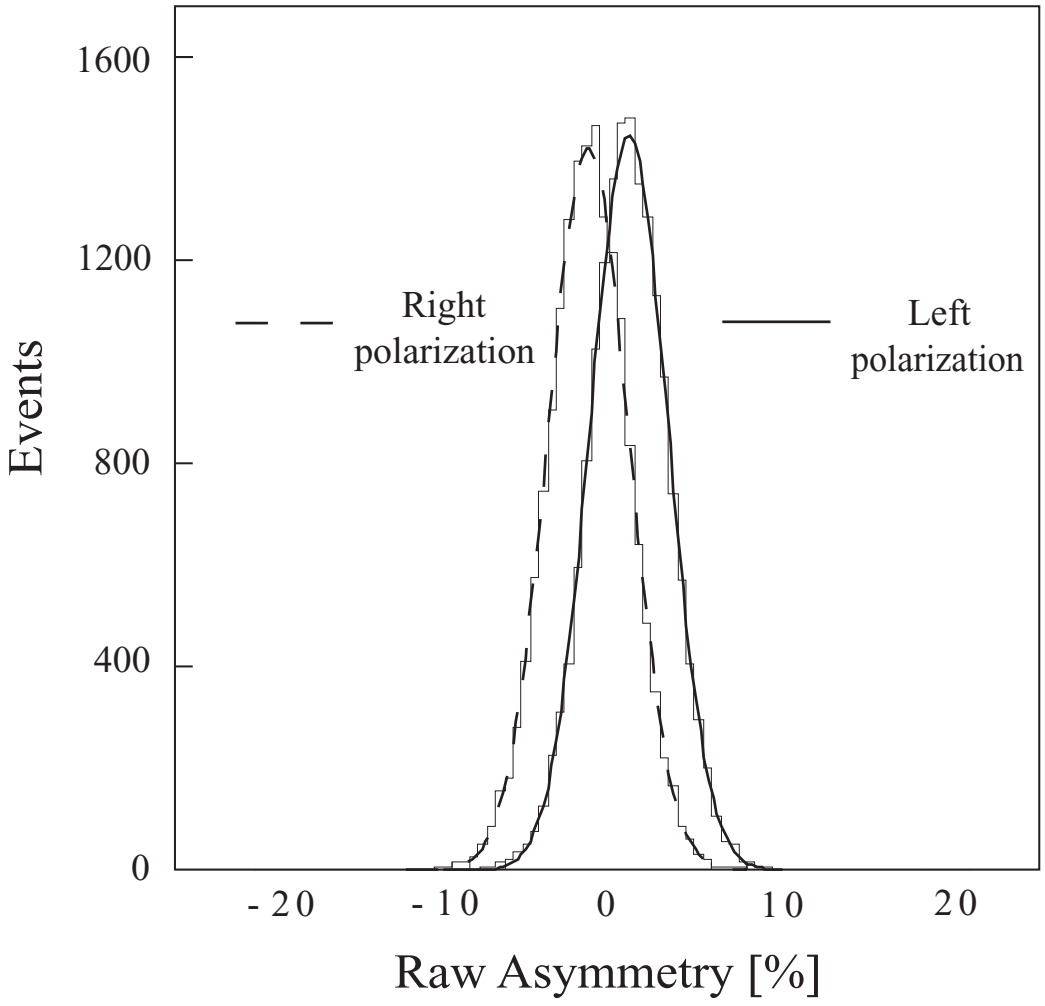

Fig. 11. *Distribution of the pulse-by-pulse experimental asymmetry obtained for the two polarization states of the photon beam.*